



HAL
open science

Delayed Inflammatory and Cell Death Responses Are Associated with Reduced Pathogenicity in Lujo Virus-Infected Cynomolgus Macaques

Angela L Rasmussen, Nicolas Tchitchek, David Safronetz, Victoria S Carter, Christopher M Williams, Elaine Haddock, Marcus J Korth, Heinz Feldmann, Michael G Katze

► **To cite this version:**

Angela L Rasmussen, Nicolas Tchitchek, David Safronetz, Victoria S Carter, Christopher M Williams, et al.. Delayed Inflammatory and Cell Death Responses Are Associated with Reduced Pathogenicity in Lujo Virus-Infected Cynomolgus Macaques. *Journal of Virology*, 2015, 89 (5), pp.2543 - 2552. 10.1128/jvi.02246-14 . hal-03851569

HAL Id: hal-03851569

<https://hal.science/hal-03851569>

Submitted on 14 Nov 2022

HAL is a multi-disciplinary open access archive for the deposit and dissemination of scientific research documents, whether they are published or not. The documents may come from teaching and research institutions in France or abroad, or from public or private research centers.

L'archive ouverte pluridisciplinaire **HAL**, est destinée au dépôt et à la diffusion de documents scientifiques de niveau recherche, publiés ou non, émanant des établissements d'enseignement et de recherche français ou étrangers, des laboratoires publics ou privés.

Delayed Inflammatory and Cell Death Responses Are Associated with Reduced Pathogenicity in Lujo Virus-Infected Cynomolgus Macaques

Angela L. Rasmussen,^a Nicolas Tchitchek,^a David Safronetz,^b Victoria S. Carter,^a Christopher M. Williams,^a Elaine Haddock,^b Marcus J. Korth,^a Heinz Feldmann,^b Michael G. Katze^{a,c}

Department of Microbiology, University of Washington, Seattle, Washington, USA^a; Laboratory of Virology, Division of Intramural Research, National Institute of Allergy and Infectious Diseases, National Institutes of Health, Rocky Mountain Laboratories, Hamilton, Montana, USA^b; Washington National Primate Research Center, Seattle, Washington, USA^c

ABSTRACT

To identify host factors associated with arenavirus virulence, we used a cynomolgus macaque model to evaluate the pathogenesis of Lujo virus (LUJV), a recently emerged arenavirus that caused an outbreak of severe viral hemorrhagic fever in southern Africa. In contrast to human cases, LUJV caused mild, nonlethal illness in macaques. We then compared this to contrasting clinical outcomes during arenavirus infection, specifically to samples obtained from macaques infected with three highly pathogenic lines of Lassa virus (LASV), the causative agent of Lassa fever (LF). We assessed gene expression in peripheral blood mononuclear cells (PBMC) and determined genes that significantly changed expression relative to that in uninfected animals over the course of infection. We detected a 72-h delay in the induction of host responses to infection during LUJV infection compared to that of the animals infected with LASV. This included genes associated with inflammatory and antiviral responses and was particularly apparent among groups of genes promoting cell death. We also observed early differential expression of a subset of genes specific to LUJV infection that accounts for the delayed inflammatory response. Cell type enrichment analysis suggested that host response induction delay and an LUJV-specific profile are due to a different proportion of natural killer cells responding in LUJV infection than that in the LASV-infected animals. Together, these data indicate that delayed proinflammatory and proapoptotic host responses to arenavirus infection could ameliorate disease severity. This conclusion provides insight into the cellular and molecular mechanisms of arenaviral hemorrhagic fever and suggests potential strategies for therapeutic development.

IMPORTANCE

Old World arenaviruses are significant human pathogens that often are associated with high mortality. However, mechanisms underlying disease severity and virulence in arenavirus hemorrhagic fever are largely unknown, particularly regarding host responses that contribute to pathogenicity. This study describes a comparison between Lujo and Lassa virus infection in cynomolgus macaques. Lujo virus-infected macaques developed only mild illness, while Lassa virus-infected macaques developed severe illness consistent with Lassa fever. We determined that mild disease is associated with a delay in host expression of genes linked to virulence, such as those causing inflammation and cell death, and with distinct cell types that may mediate this delay. This is the first study to associate the timing and directionality of gene expression with arenaviral pathogenicity and disease outcome and evokes new potential approaches for developing effective therapeutics for treating these deadly emerging pathogens.

Since their discovery in the early 20th century, arenaviruses have been consistently associated with outbreaks of severe illness, including viral hemorrhagic fever (VHF) and encephalitis. Arenaviruses are bisegmented, ambisense, single-stranded, negative-sense RNA viruses typically carried by rodents and named for their areas of origin. In 2008, a novel arenavirus, Lujo virus (LUJV), was associated with an outbreak of VHF in southern Africa with a case fatality rate of 80% in 5 human cases. The symptoms of LUJV VHF were similar to those of severe Lassa fever (LF), including rash, headache, myalgia, respiratory distress, neurological symptoms, renal failure, and circulatory collapse (1). LUJV was determined to be a phylogenetically distinct member of the family *Arenaviridae*, branching from the ancestral node of the Old World arenaviruses (2). Although additional cases of LUJV have not been reported since the initial outbreak and the reservoir species remains unknown, the development of an experimental model of VHF caused by LUJV is desirable to prevent and treat future human cases and to compare it with other related infections, such as the prototypical Old World arenaviral hemorrhagic fever pathogen Lassa virus (LASV).

LASV, the causative agent of LF, is endemic in western Africa and causes as many as 500,000 cases per year. The natural reservoir of LASV is *Mastomys natalensis*, and transmission occurs largely through contaminated rodent excreta (1, 3). In humans, LASV infection produces acute infection with a wide spectrum of clinical

Received 4 August 2014 Accepted 1 December 2014

Accepted manuscript posted online 17 December 2014

Citation Rasmussen AL, Tchitchek N, Safronetz D, Carter VS, Williams CM, Haddock E, Korth MJ, Feldmann H, Katze MG. 2015. Delayed inflammatory and cell death responses are associated with reduced pathogenicity in Lujo virus-infected cynomolgus macaques. *J Virol* 89:2543–2552. doi:10.1128/JVI.02246-14.

Editor: B. Williams

Address correspondence to Michael G. Katze, honey@uw.edu.

A.L.R., N.T., and D.S. contributed equally to this publication.

Supplemental material for this article may be found at <http://dx.doi.org/10.1128/JVI.02246-14>.

Copyright © 2015, American Society for Microbiology. All Rights Reserved.

doi:10.1128/JVI.02246-14

manifestations, ranging from asymptomatic or mild, subclinical disease to severe, lethal VHF. During LF epidemics, case fatality rates can approach 50% (4, 5). Despite the prevalence of LASV in areas where it is endemic and the severity of disease during outbreaks, factors contributing to pathogenicity and virulence still are poorly characterized on account of the remote areas of endemicity and disease epidemiology complicated by secondary nosocomial transmission. Comparative analyses of different models of arenavirus VHF may provide critical insights into the host factors that determine disease severity.

An experimental model of LASV pathogenesis in cynomolgus macaques (*Macaca fascicularis*) is established and reproduces a number of clinical features of human VHF, including fever, hemorrhage, multiorgan failure, and eventual death (6–8). However, recently a *Mastomys* isolate from southern Mali (Soromba-R) was found to be less pathogenic than historical isolates, causing reduced mortality and unusual clinical presentation in cynomolgus macaques (9). We observed that, unlike human patients, cynomolgus macaques are not susceptible to severe disease following LUJV infection, developing a mild, transient illness that completely resolves with no mortality. The first goal of the study was to determine the virulence of LUJV in macaques. Once we found that it caused only a mild disease, we then had the opportunity to compare the host response to LUJV with that to an arenavirus (LASV) that causes severe disease in macaques.

MATERIALS AND METHODS

Animal work and biosafety. Animal experiments were approved by the Institutional Animal Care and Use Committee of Rocky Mountain Laboratories (RML) and were performed in accordance with guidelines established by the Association for Assessment and Accreditation of Laboratory Animal Care (AAALAC) by certified staff in an AAALAC-accredited facility. Experiments were conducted in the biosafety level 4 (BSL-4) laboratory at RML with the approval of the RML Institutional Biosafety Committee (IBC). Sample inactivation was performed according to standard operating procedures approved by the IBC for removal of specimens from BSL-4 containment.

Viruses. Low-passage (defined as <4 passages) LASV isolates Josiah (LASV_{Jos}) (10), Z-132 (LASV_{Z132}) (11, 12), and Soromba-R (LASV_{Sor}) (11), as well as LUJV, were cultured in Vero cells and titrated using standard methods for determining the median tissue culture infective dose (TCID₅₀).

Infection and sampling protocol. Cynomolgus macaques (*Macaca fascicularis*) were infected with 1×10^4 TCID₅₀ of LASV_{Jos}, LASV_{Z132}, LASV_{Sor}, or LUJV by intramuscular injection ($n = 3$ animals per condition). Animals were monitored twice daily and assigned a numerical score based on clinical signs of disease, including posture, respiration, feces/urine production, food intake, behavior/attitude, skin turgor, fever, and recumbency, using an approved endpoint scoring sheet. On days –7, 0, 1, 3, 7, 10, and 14, animals were examined under anesthesia, and chest radiography was performed, pulse rate, blood pressure, temperature, and respiration rates were measured, and animals were bled for analysis of blood chemistry, coagulation parameters, differential blood counts, virologic characteristics, cytokine profiling, and isolation of peripheral blood mononuclear cells (PBMC). Animals were euthanized by exsanguination under deep anesthesia when clinical scores exceeded 30, which is indicative of terminal disease (13).

RNA extraction, probe synthesis, and microarray hybridization. PBMC were isolated on a Ficoll gradient, washed with phosphate-buffered saline, suspended in equal volumes of AVL buffer (Qiagen, Valencia, CA) and 70% ethanol, and stored at –80°C until preparation. Samples were thawed, and two additional volumes of buffer RLT (Qiagen, Valencia, CA) with 0.01 volumes of 2-mercaptoethanol were added, followed by

an additional two volumes of 70% ethanol. RNA then was extracted using Qiagen microRNeasy spin columns per the manufacturer's protocol. Low-yield samples were concentrated using the RNA Clean and Concentrator (Zymo Research, Irvine, CA). Probe labeling was carried out using the Agilent low-input processing protocol and hybridized to Agilent rhesus macaque 4x44K microarrays (Agilent Technologies, Santa Clara, CA) using the manufacturer's one-color analysis protocol.

Microarray analysis. Transcriptomics data were extracted from the Agilent rhesus macaque gene expression microarray raw data and scale normalized (14–16) using the “normalizeBetweenArrays” normalization method available in the limma package (17) of the R suite (18).

Transcriptomic raw data are available at <http://viromics.washington.edu/> and the NCBI GEO database (19) under accession number GSE49838.

Differentially expressed genes were identified using the CDS method (20). The CDS statistical test allows the identification of differentially but also similarly expressed genes between two biological conditions using a statistical hypothesis test that formulates fold change statements. A fold change of 1.2 was used as a parameter for the statistical test, and a *P* value cutoff of 0.05 was used to identify significantly differentially expressed genes, as these are commonly used statistical thresholds for microarray experiments.

For each infection condition, pairwise comparisons between each series of gene expression profile were performed using the Pearson's coefficient of correlation. Genes having a pairwise comparison coefficient of less than 0.60 were excluded.

Functional analysis was performed using Ingenuity pathway analysis (IPA; Ingenuity Systems, Inc.). IPA examines differentially expressed transcripts and proteins in the context of known functions, mapping each gene identifier to its corresponding molecule in the Ingenuity pathways knowledge base (IPKB). For all analyses, the *P* values were generated using the right-tailed Fisher's exact test (21) and adjusted using the Benjamini-Hochberg multiple-testing correction (22).

RT-PCR for viral genomes. RNA was reverse transcribed using the QuantiTect kit (Qiagen), and viral genomes were quantitated by TaqMan quantitative real-time reverse transcription-PCR (RT-PCR) using rhesus macaque GMP reductase 2 (GMPR2; TaqMan assay ID Rh01076490_m1; Life Technologies) as the endogenous control. For quantifying viral genomes, we used the following primer/probe sets: LASV_{Jos} forward primer, 5'-TGCTAGTACAGACAGTGCAATGAG-3'; reverse primer, 5'-TAGTGACATTCTCCAGGAAGTGC-3'; probe, 6-FAM-5'-TCTGC GGAACCGGTG-3'-MGBNFQ (6-FAM stands for 6-carboxyfluorescein, and MGBNFQ stands for molecular groove-binding nonfluorescence quencher); LASV_{Z132} forward primer, 5'-CCCCAAACAATGGATGGT ATTCTCA-3'; reverse primer, 5'-CTTTCACCAGGAGTGTCCGA AATAA-3'; probe, 6-FAM-5'-CATCCCAAGAGCTTTC-3'-MGBNFQ; LASV_{Sor} forward primer, 5'-ACTTTAGTTTGGGTGCTGCAGT-3'; reverse primer, 5'-CCAACATGTTCCACCATCCAA; probe, 6-FAM-5'-ACAGGCACCTGCTTTT-3'-MGBNFQ; LUJV forward primer, 5'-ATT TAAGTCCACCAAGCCA-3'; reverse primer, 5'-CGTGAGAGCCAAA GTTGTCA-3'; probe, 6-FAM-5'-TGCCGTGAGTCTGATCAACGGCC T-3'-MGBNFQ.

We normalized the values using primer-probe sets for the endogenous control macaque GMPR2 RNA per the manufacturer's specifications (Life Technologies). All reactions were performed using standard TaqMan protocols and reagents supplied by the manufacturer and run on an ABI 7500 real-time PCR instrument (Life Technologies).

Multidimensional scaling. Multidimensional scaling representations were generated using the singular value decomposition-multidimensional scaling (SVD-MDS) method (23). Multidimensional scaling methods represent the similarities and differences among high-dimensionality objects into a space having a low number of dimensions, usually in 2 or 3 dimensions, for visualization. Pairwise distances between the dots are proportional to the transcriptomic distances between the samples and were calculated using the Euclidian metric. The Kruskal stress criterion

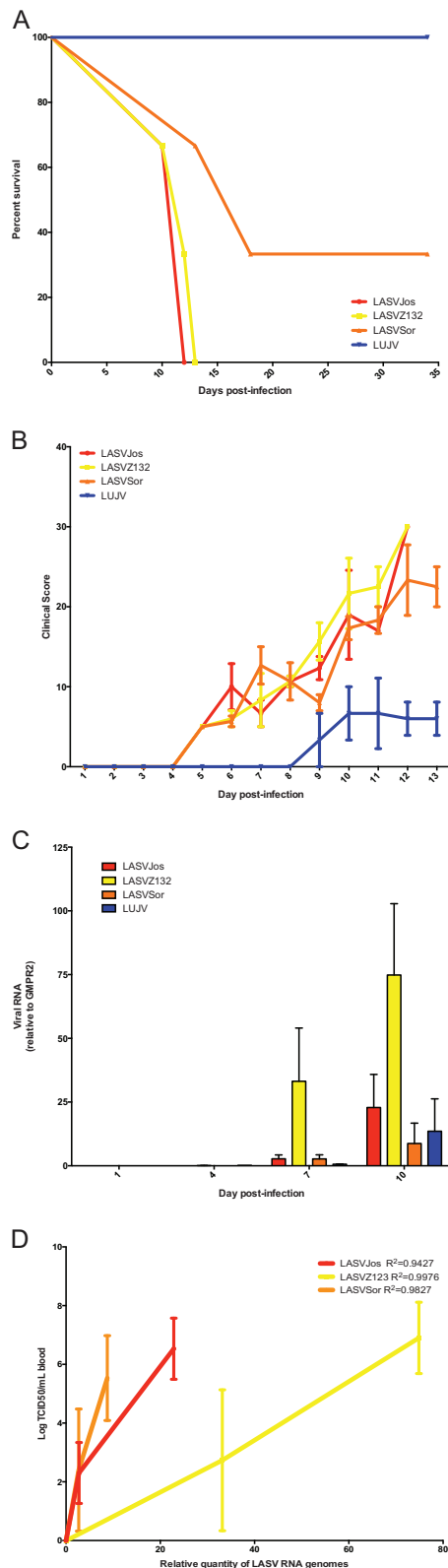


FIG 1 Pathogenesis of LASV isolates and LUJV in infected macaques. (A) Kaplan-Meier survival curve depicting mortality over the course of infection for LASVJos (red line), LASVZ132 (yellow line), LASVSor (orange line), and LUJV (blue line). (B) Clinical score of individual animals over the course of infection as determined by observed clinical signs of disease, including abnormal posture, respiration, feces/urine, food intake, and behavior/attitude, as

(24) shown quantifies the quality of the representation as a fraction of the information lost during the dimensionality reduction procedure.

Cell type enrichment analysis. The functional enrichment of cell type was done based on the Human Gene Atlas data set (25) and computed using Enrichr (26). The Human Gene Atlas data set consists of whole-genome protein-coding transcript expression measurements across a diverse panel of 79 human tissues. Enrichr is a web-based enrichment analysis tool allowing rank-based comparisons of gene signatures with a large variety of -omics metadata sets.

Radar chart representations were generated using the “radarchart” method of the “fmsb” package (<http://cran.r-project.org/web/packages/fmsb/index.html>) of the R suite. *P* values of the cell type enrichments obtained from Enrichr were $-\log_{10}$ transformed and then represented in the radar charts.

Microarray data accession number. The transcriptomics data determined in the course of this work were deposited in the NCBI GEO database (19) under accession number GSE49838.

RESULTS

LUJV infection produces mild disease in cynomolgus macaques.

As LUJV pathogenesis has not been evaluated in a nonhuman primate model, we first determined the pathogenic phenotype of LUJV in cynomolgus macaques relative to LASV-infected animals using the same infection protocol and sampling schedule. We sought to compare LUJV infection with previously published data from three distinct strains of LASV following inoculation by intramuscular injection. We previously evaluated the pathogenicity of three different isolates of LASV, comparing a more recent isolate from southern Mali, Soromba-R, to two historical isolates from Sierra Leone (Josiah) and Liberia (Z-132). The Soromba-R isolate (LASVSor) was found to be less virulent in both guinea pig and cynomolgus macaque models of infection than the Josiah (LASVJos) or Z-132 (LASVZ132) viruses, with LASVSor showing a slower progression to death, delayed disruptions in coagulation profiles, a lack of observable febrile disease, and a 57% mortality rate. We observed clinical manifestations of disease in 1/3 of the surviving LASVSor-infected animals used in this study (67% mortality) and delayed progression to severe VHF compared to the uniformly lethal disease in animals infected with LASVJos and LASVZ132 isolates (9). However, all animals infected with LUJV survived infection (Fig. 1A). Furthermore, LUJV-infected animals had mild disease with no evidence of hemorrhage or disrupted coagulation, and clinical scores for the LUJV animals were lower throughout the course of infection compared to those for the LASV-infected animals (Fig. 1B). Complete clinical data for each animal over the course of infection are available in Table S1 in the supplemental material.

Viral infection and microarray analysis of PBMC. We used microarrays to monitor transcriptional profiles of macaque PBMC following infection with LUJV. We collected PBMC longitudinally over a time course of 29 days. In addition, we determined transcriptional profiles from PBMC collected from 3 uninfected macaques for use as a control. To compare the LUJV-associated

as well as skin turgor, fever, and recumbency, as described in Materials and Methods. (C) Relative expression of viral genomes in PBMC over the course of infection by quantitative RT-PCR. Genomic RNA is expressed relative to GMPr2 mRNA. Groups of 3 animals were assessed for each infection condition. (D) Pearson’s correlation between LASV 50% tissue culture infectious doses in whole blood and relative LASV RNA genome quantities in PBMC at days 4 to 10 postinfection.

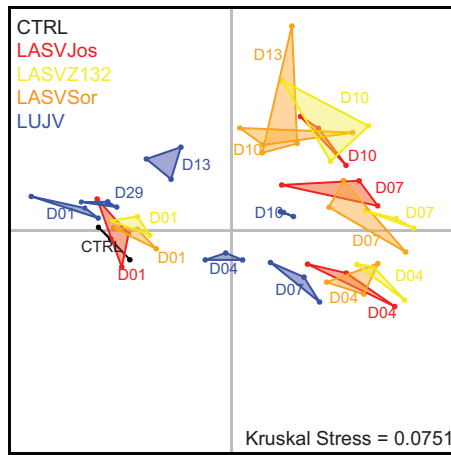


FIG 2 Kinetics of PBMC transcriptional responses to LASV and LUJV infection. Multidimensional scaling (MDS) representation of the transcriptomic profiles of LASV- and LUJV-infected samples. Each dot represents a transcriptomic profile from an individual biological sample plotted in the intensity space of gene expression signals. Pairwise distances between the dots are proportional to the transcriptomic distances between the samples. Transcriptomic distances were calculated based on the signature of genes associated with the kinetics of the host response following infection. Samples ($n = 3$ per condition) are colored to indicate different infection conditions (uninfected control [CTRL], black; LASVJos, red; LASVZ132, yellow; LASVSor, orange; LUJV, blue), and biological conditions are indicated by the convex hull of the set of biological replicates and labeled to indicate the time point postinfection. Later time points were analyzed only if a full set of 3 replicate samples were available. The Kruskal stress shown in each representation quantifies the quality of the geometrical representation as a fraction of the information lost during the dimensionality reduction procedure.

transcriptional response with the more pathogenic LASV isolates in infected cynomolgus macaques, we also performed analysis on PBMC banked from the earlier LASV study (9). PBMC were selected for these studies, as this allowed us to perform longitudinal measures on the same animals throughout the course of infection, and PBMC are comprised of immune cell types that are known to be infected with arenaviruses and involved in the pathogenesis of LF and VHF (27). Immune responses are thought to heavily influence the course of LASV pathogenesis, and some monocyte-derived cells, such as DCs and macrophages, are susceptible to LASV infection, which perturbs cellular functions, such as antigen presentation, lymphocyte activation, and cytokine secretion (28). We observed increasing virus levels in PBMC late in infection for all four viruses evaluated (Fig. 1C), which indicates that transcriptional differences are not substantially attributed to large differences in viral replication in these cells.

Host response kinetics during LASV and LUJV infection. In order to analyze the kinetics of the host responses in PBMC following infection of macaques with LUJV, we compared transcriptomic data to that from LASV-infected macaques. We identified differentially expressed genes (DEG) in at least one infection condition compared to uninfected controls, in which expression was correlated with time for each virus. We identified a signature of 646 genes significantly associated with the dynamics of host gene expression over the course of infection (see Table S2 in the supplemental material). To assess overall transcriptional differences between different viruses over time, we performed multidimensional scaling (MDS) on transcriptomic profiles restricted to this list of 646 genes (Fig. 2). This method simplifies visualization by

reducing the complex, multidimensional kinetics-associated gene signature to a two-dimensional representation. Over the course of infection, the three LASV isolates showed overlapping profiles, indicating that these genes were expressed similarly in terms of direction and magnitude. In contrast, LUJV infection produced transcriptionally distinct signatures after day 1 postinfection. The LUJV day 7 and day 10 samples were more similar to the LASV day 4 and day 7 samples, respectively, suggesting that LUJV induced genes associated with disease progression at a lower rate than did LASV. The LUJV-induced profile followed a circular trajectory, beginning and ending at similar positions, indicating that at day 29 the samples returned to transcriptional baseline. This follows the course of disease in the animals, and the final position likely reflects the animals' complete resolution of infection and return to baseline levels of gene expression. However, the slight positional separation of LUJV from the LASV profiles at day 1 indicates that there is an LUJV-specific transcriptional response to infection very early postinfection.

Using IPA, we investigated the functional enrichment of the kinetic profile for each condition. Not surprisingly, well-studied antiviral innate immune responses constituted the top five most significant IPA canonical pathways, including interferon signaling, communication between innate and adaptive immune cells, role of pattern recognition receptors in recognition of bacteria and viruses, antigen presentation, and activation of interferon regulatory factors (IRF) by cytosolic pattern recognition receptors. These genes were induced at day 1 postinfection and were increasingly expressed over the course of infection for all viruses investigated, suggesting that the animals all mounted typical antiviral responses against both LASV and LUJV infection, including upregulation of interferon-stimulated genes. Therefore, the differences in clinical outcomes between LASV and LUJV must be associated with other aspects of the host response.

A notable distinction between the response to LUJV and the three LASV isolates was the differential induction of genes associated with cell death, as characterized by transcriptional programs promoting apoptosis as well as more general mechanisms of cell death, such as necrosis. We examined the average z scores predicted by IPA for activation state within various functional categories. On day 1 postinfection, pathways related to cell death were inhibited in LUJV-infected animals (as indicated by negative-activation z scores) compared to levels for all three LASV groups, in which these categories were activated (Fig. 3A). Specifically, LUJV-infected animals at day 1 showed a high degree of inhibition associated with multiple cell death functional categories, including cell death of lymphoid organs, cell death of immune cells, cell death of blood cells, cell clearance, removal of cells, and cytolysis. Concurrently, these animals showed increased activation of functions resulting in the delay of cell death in myeloid cells, phagocytes, and leukocytes (Fig. 3B). Another notable difference at day 1 was the induction of mast cell apoptosis in LUJV-infected animals compared to that of LASVZ132- and LASVSor-infected animals, which inhibited this process. This demonstrates that while cell death inhibition was not absolute in LUJV-infected animals, the response still was functionally distinct from that observed in LASV-infected animals. However, by day 4, genes associated with cell death were induced in LUJV-infected animals, similar to what was seen in the LASV-infected groups (Fig. 3A). This initial lag in cell death induction indicates the basis for distinct

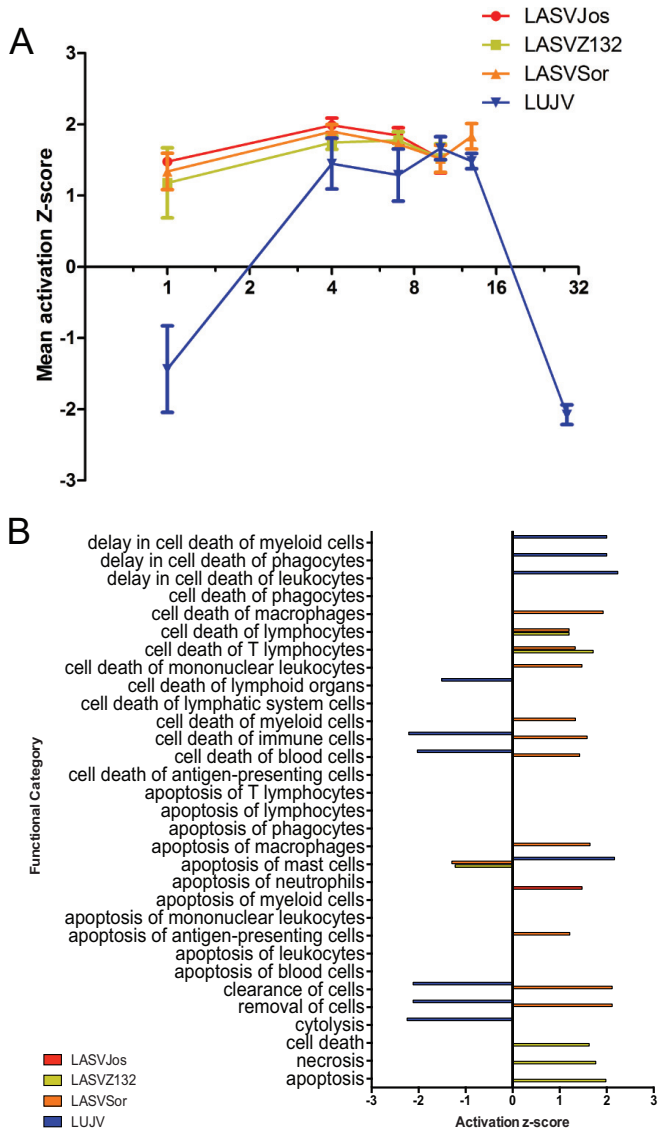


FIG 3 Enrichment of functional categories associated with cell death. (A) Mean activation z scores of functional categories associated with cell death for gene expression signatures associated with each infection condition (LASVJos, red; LASVZ132, yellow; LASVSor, orange; LUJV, blue). (B) Individual cell death functional categories with activation z scores exceeding 1.2 at day 1 postinfection.

cellular responses that contribute to disease severity and progression of VHF.

Early LUJV-specific gene signatures associated with control of arenavirus pathogenesis. Because of the clear difference in host response kinetics between LUJV-infected animals and LASV-infected animals, we sought to determine differential signatures unique to LUJV early in the course of infection, before any clinical indications of disease were observed, by identifying DEG only at day 1 postinfection that are specific to LUJV infection. We reasoned that early gene expression profiles programmatically define host responses associated with the less pathogenic disease course of LUJV infection rather than the severe and mostly fatal VHF disease consequent to LASV infection in this model. Thus, we investigated the genes specific to the LUJV host response at the

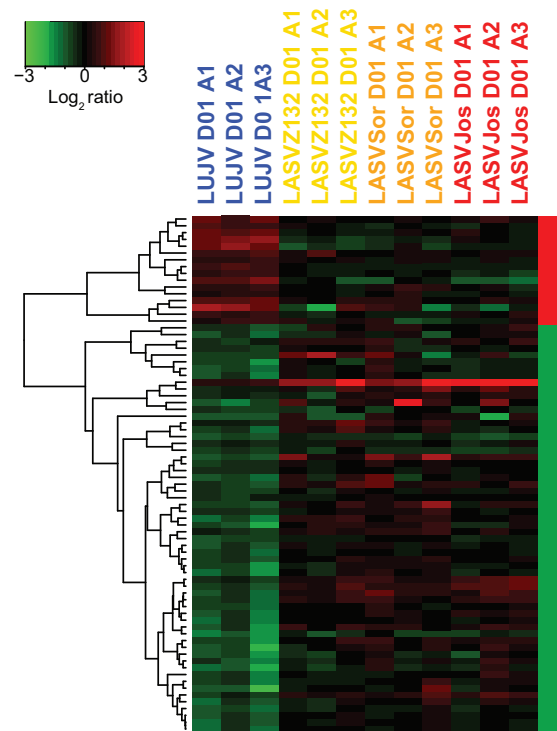


FIG 4 Genes specific to LUJV compared to LASV at the earliest time point postinfection. Heatmap and dendrogram showing the ratio of gene expression values to those of the control samples for each biological replicate at 1 day postinfection. The heatmap has been restricted to genes identified as specific to LUJV at 1 day postinfection. Hierarchical clustering was performed using the Pearson's coefficient of correlation of gene expression profiles and using a single linkage. The bar to the right of the heatmap shows upregulated and downregulated genes.

earliest time point postinfection. Based on the previously identified kinetic gene signature, we identified the subset of genes that were both differentially expressed in LUJV animals compared to controls and differentially expressed between the LUJV and LASV infection conditions. We identified 76 DE genes (17 upregulated and 59 downregulated) specific to LUJV infection at 1 day postinfection (see Table S3 in the supplemental material) and examined these gene expression values relative to those of the uninfected controls for each biological replicate collected at 1 day postinfection (Fig. 4). These genes were predominantly related to cellular growth, differentiation, and migration, particularly in white blood cells. In particular, inflammatory white blood cell responses were inhibited, including protein synthesis, cell division, and immune cell chemotaxis. Gene expression associated with these processes later increased during LUJV infection, consistent with a delayed host response in LUJV infection compared to animals infected with LASV.

Cell type composition analysis reveals LUJV-specific early induction of NK cells. Because PBMC are comprised of multiple immune cell types and the relative proportions of these can vary greatly between individuals, we sought to determine the specific cell types driving distinct transcriptional responses to each virus. While we were able to determine total numbers of different classes of cells (Fig. 5; also see Table S1 in the supplemental material), this analysis allows us to determine which specific cell types are driving the transcriptional responses. We performed enrichment analysis

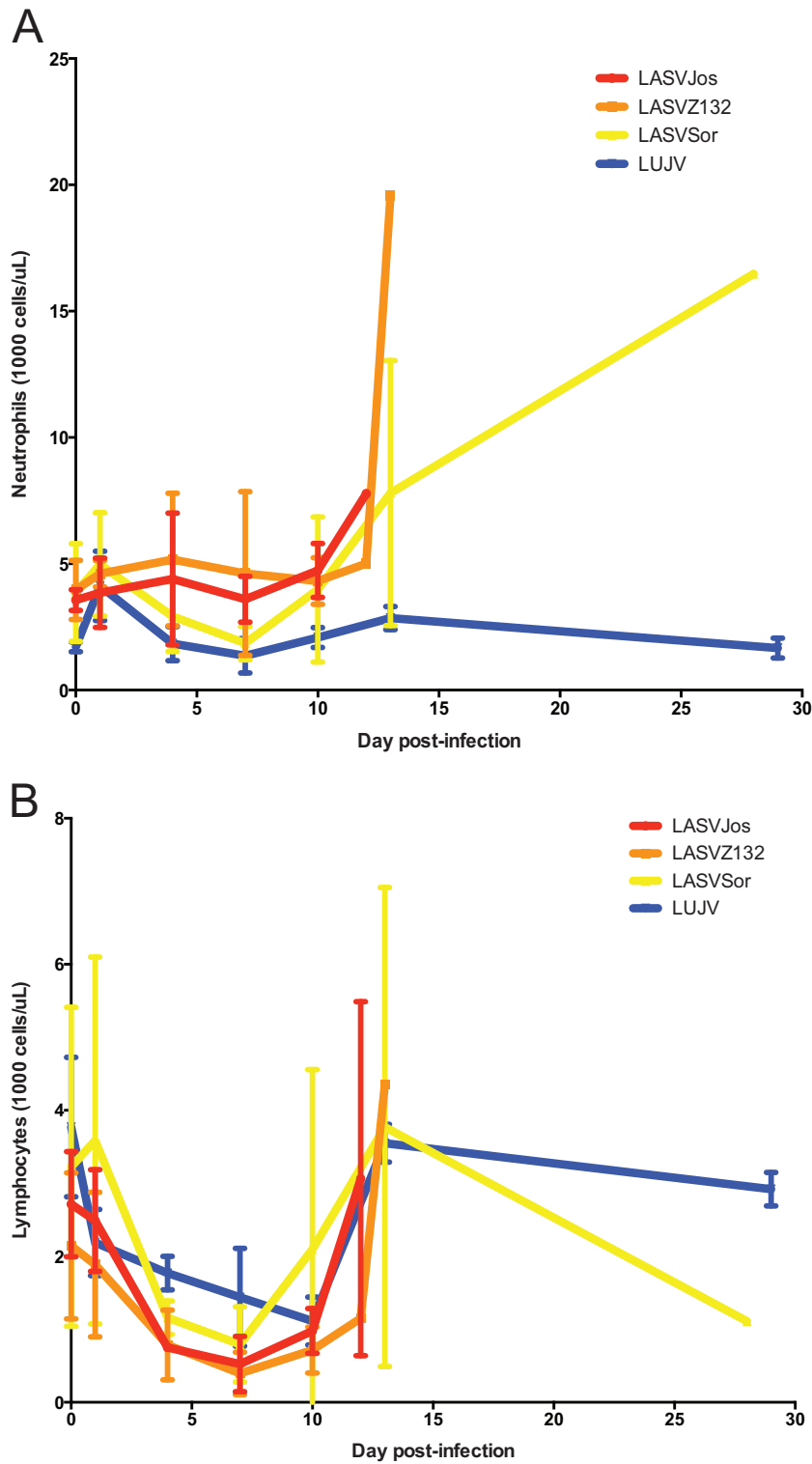


FIG 5 Total white blood cell subsets throughout course of arenavirus infection. The quantity of neutrophils (A) and lymphocytes (B) enumerated in whole blood over the course of infection is shown.

using a meta-data set of gene expression measurements obtained from a diverse panel of 79 human tissues (25). For each list of differentially expressed genes, we identified the most significant overlaps with cell type-specific transcriptome profiles (Fig. 6).

Concordant with clinical symptoms, all four viruses induced significant enrichment in the expression of genes associated with CD14⁺ monocytes and CD33⁺ myeloid cells at days 4 to 13 postinfection, with the greatest enrichment occurring at days 10 to

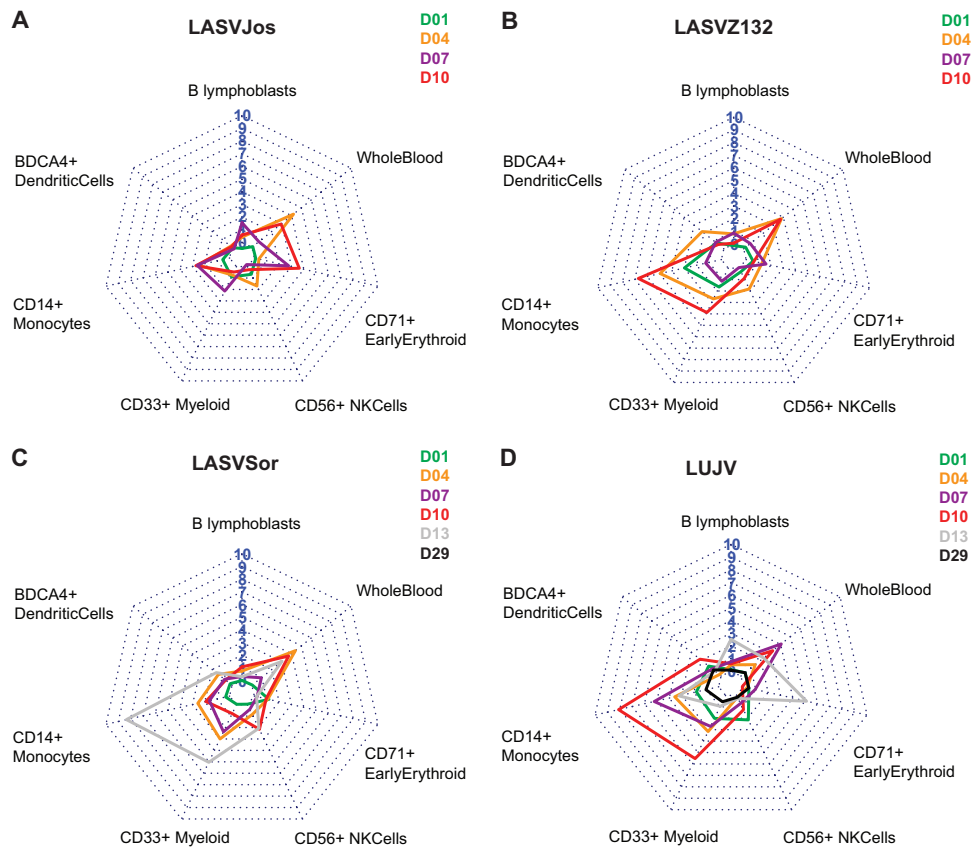


FIG 6 Immune cell type compositions of LASV- and LUJV-infected PBMC. Radar chart representations showing the functional enrichment of immune cell types for the different lists of differentially expressed genes during infection with LASVJos (A), LASVSor (B), LASVZ132 (C), and LUJV (D). Radar charts represent multivariate data in the form of quantitative variables depicted on axes starting from the same point. Each spoke radiating from the center of the plot represents the functional enrichment, shown as $-\log_{10}(P \text{ value})$, for a given day postinfection and a given immune cell type. The length of a spoke is proportional to the magnitude of the functional enrichment; lower enrichment values are represented close to the center of the representations, while higher enrichment values are represented close to the borders of the representations. Spokes of the same gene signature are connected with lines and colored in order to indicate the time point postinfection.

13, coincident with peak viremia. Antigen-presenting cells (APC) are thought to be primary targets of LASV infection (28, 29), and this enrichment may reflect increased mobilization of infected monocytic and myeloid lineage cells in the blood.

We also observed that PBMC from LUJV-infected macaques showed enrichment of genes associated with CD56⁺ natural killer (NK) cells (Fig. 6D) at day 1 postinfection compared to the LASV isolates studied. The enrichment scores for all three LASV isolates were at least 3-fold lower than those for LUJV, suggesting that at early time points, LUJV mobilized NK cells, which may have important consequences for immunity. Lethal LASV infection previously has been associated with early leukopenia, including lower NK cell counts (30). However, the mechanism for this is unclear, as human NK cells in culture are not susceptible to LASV infection despite being activated by LASV-infected APCs (31). We also observed increased enrichment of genes associated with B lymphoblasts at day 13 in LUJV-infected animals, suggesting that functional B cell responses are associated with the control of LUJV pathogenicity late in infection. Concurrent with this, we observed differentially upregulated genes associated with B lymphocyte proliferation and maturation, including genes associated with isotype switching and differentiation (activation-induced cytidine deaminase [AICDA], interleukin-4 [IL-4], and tumor necrosis

factor ligand superfamily member 13B [TNFSF13B]). It is not clear how these results would correlate with antibody production or other measures of B cell function. Antibodies are produced early in LASV infection in human patients, although these likely are not neutralizing (32). Low titers of neutralizing IgG are produced a month after acute LASV infection (33), and accompanying early cellular immune responses are associated with control of infection and recovery in cynomolgus macaques (30). Therefore, the induction of B cell responses in LUJV-infected animals at day 13 postinfection may represent a component of a more robust cellular immune response that ultimately controls disease progression.

DISCUSSION

This study was initiated to determine if *M. fascicularis* is a suitable experimental model for studying LUJV pathogenesis, since the cynomolgus macaque has been used successfully for modeling LF pathogenesis (6, 9). Additionally, this model has been used to make direct comparisons with human cells in determining immune responses to LASV infection (34). Although we found that LUJV infection in macaques did not produce severe disease similar to that observed in human cases, the evident ability of the animals to limit virulence despite similar levels of viral RNA pro-

duction (Fig. 1C) compared to LASV indicates that LUJV induces a transcriptional response that limits pathogenesis and progression to lethal hemorrhagic fever. We observed a striking down-regulation of genes specific to LUJV infection at day 1 postinfection, as well as a general delay in transcription following infection compared to LASV-infected animals. This was similar to delays in differential gene expression induction observed in PBMC from macaques infected with nonvirulent lymphocytic choriomeningitis virus (LCMV) compared to virulent LCMV prior to observable viremia (35). Together, these data suggest that the postponement of specific host responses contributes to a milder pathogenic phenotype and survival. Notably, the delay of cell death-related pathways may contribute to improved survival of distinct populations of immune cells, which in turn can alter pathogenesis in the host. The specific induction of mast cell apoptosis early following LUJV infection may partly explain the milder pathology, as mast cells have been associated with inflammatory pathology in response to virus infection (36–44), including vascular leakage associated with dengue hemorrhagic fever (45). The early selective depletion of mast cells may account for immune responses associated with controlled antiviral responses rather than uncontrolled inflammation and consequent mild disease during LUJV infection.

The basis for this delay during LUJV infection is not altogether clear. Viral RNA is detectable in LUJV-infected and LASV-infected animals at the same time point, indicating that there is little difference in the time course and magnitude of viral RNA production in the blood (Fig. 1C). Thus, it is likely that the reduced pathogenicity observed in LUJV-infected animals is due to distinctive host responses rather than a lower level of viral replication, although we cannot rule out the possibility that these animals are producing lower levels of infectious virus. We are not able to assay for infectious LUJV, although LASV infectious serum titers correlated with levels of viral RNA in PBMC (Fig. 1D). We also cannot rule out the possibility that we would have observed a more significant disease in the LUJV-infected animals with a different virus inoculum.

Prior to this study, very few attempts have been made to profile gene expression changes associated with Old World arenavirus infection in nonhuman primates. Studies using both LASV and LCMV have observed activation of antiviral and immune responses, with a concurrent inhibition of classical proinflammatory pathways in rhesus and cynomolgus macaque infection models (4, 35, 46). Notably, delays in gene expression in PBMC were associated with nonvirulent LCMV infection (35). However, this study is the first to directly compare highly pathogenic arenaviruses with various levels of pathogenicity in a nonhuman primate model and to associate transcriptional kinetics with pathogenic outcome. We were surprised that we did not observe greater differences between LASV and the other, more pathogenic LASV isolates included in this comparison, particularly when LASV was previously observed to have distinct pathology and inflammatory responses (9). We suspect that this is because either these responses are not regulated at the transcriptional level or because the PBMC are not driving the distinct pathological responses that distinguish these different LASV isolates. The delay in transcriptional responses associated with LUJV could indicate future therapeutic strategies for treating VHF caused by emerging arenaviruses. In particular, drugs that induce a delay in host responses to infection or suppress host responses to infection could reduce pathogenic effects. Because the delay in responses to LUJV occurs

early in infection, it may be impractical to administer host response modulators in patients who have progressed to symptomatic disease. This type of treatment strategy could be used as an effective countermeasure, however, in cases of suspected exposure or to control spread in an outbreak setting.

Although human transcriptional responses to LUJV have not been characterized, we hypothesize that these responses would be more similar to the more highly pathogenic LASV isolates. Future studies should address LUJV responses specific to known cellular targets of arenavirus infection using human macrophage lines or donor PBMC *ex vivo* to determine whether human responses to LUJV are similar to those elicited by LASV infection in macaques. In particular, studies should address whether distinct cellular tropism, possibly caused by distinct receptor usage or variable susceptibilities, in different PBMC cell types account for differential virulence in macaques. Such an experimental system then could be applied to screen for compounds that would induce delayed responses similar to those observed in LUJV-infected macaques in this study. This would also increase confidence in the data obtained from the macaques, which are variable and limited to small group sizes due to logistics and cost. Additionally, this could be used to address questions of the timing of treatment with immunomodulatory host-directed drugs. Treatment with drugs that would delay and attenuate human responses, and induce those similar to LUJV infection in the macaques, could reduce disease severity and improve patient outcomes. For viruses such as LUJV, which emerged unexpectedly in human populations with a high case fatality rate, countermeasures that can modulate or delay host transcriptional responses may represent a useful new paradigm for treating uncharacterized and highly virulent emergent viruses.

ACKNOWLEDGMENTS

This study was supported in part by awards P51 OD010425, U54 AI081680, and U19 AI109761 from the National Institute of Allergy and Infectious Diseases and by the Intramural Research Program of the National Institute of Allergy and Infectious Diseases, National Institutes of Health.

REFERENCES

- Shaffer JG, Grant DS, Schieffelin JS, Boisen ML, Goba A, Hartnett JN, Levy DC, Yenni RE, Moses LM, Fullah M, Momoh M, Fonnies M, Fonnies R, Kanneh L, Koroma VJ, Kargbo K, Ottomassathien D, Muncy IJ, Jones AB, Illick MM, Kulakosky PC, Haislip AM, Bishop CM, Elliot DH, Brown BL, Zhu H, Hastie KM, Andersen KG, Gire SK, Tabrizi S, Tariyal R, Stremmler M, Matschiner A, Sampey DB, Spence JS, Cross RW, Geisbert JB, Folarin OA, Happi CT, Pitts KR, Geske FJ, Geisbert TW, Saphire EO, Robinson JE, Wilson RB, Sabeti PC, Henderson LA, Khan SH, Bausch DG, Branco LM, Garry RF, Viral Hemorrhagic Fever Consortium. 2014. Lassa fever in post-conflict Sierra Leone. *PLoS Negl Trop Dis* 8:e2748. <http://dx.doi.org/10.1371/journal.pntd.0002748>.
- Briese T, Paweska JT, McMullan LK, Hutchison SK, Street C, Palacios G, Khristova ML, Weyer J, Swanepoel R, Egholm M, Nichol ST, Lipkin WI. 2009. Genetic detection and characterization of Lujo virus, a new hemorrhagic fever-associated arenavirus from southern Africa. *PLoS Pathog* 5:e1000455. <http://dx.doi.org/10.1371/journal.ppat.1000455>.
- Buchmeier M, de la Torre J, Peters C. 2007. Arenaviridae: the viruses and their replication, p 1791–1827. In Knipe DM, Howley PM, Griffin DE, Lamb RA, Martin MA, Roizman B, Straus SE (ed), *Fields virology*, 5th ed. Lippincott Williams & Wilkins, Philadelphia, PA.
- Fisher-Hoch SP, Tomori O, Nasidi A, Perez-Orozco GI, Fakile Y, Hutwagner L, McCormick JB. 1995. Review of cases of nosocomial Lassa fever in Nigeria: the high price of poor medical practice. *BMJ* 311:857–859. <http://dx.doi.org/10.1136/bmj.311.7009.857>.
- McCormick JB, Webb PA, Krebs JW, Johnson KM, Smith ES. 1987. A

- prospective study of the epidemiology and ecology of Lassa fever. *J Infect Dis* 155:437–444. <http://dx.doi.org/10.1093/infdis/155.3.437>.
6. Hensley LE, Smith MA, Geisbert JB, Fritz EA, Daddario-DiCaprio KM, Larsen T, Geisbert TW. 2011. Pathogenesis of Lassa fever in cynomolgus macaques. *Virology* 420:8–205. <http://dx.doi.org/10.1186/1743-422X-8-205>.
 7. Jahrling PB, Peters CJ. 1984. Passive antibody therapy of Lassa fever in cynomolgus monkeys: importance of neutralizing antibody and Lassa virus strain. *Infect Immun* 44:528–533.
 8. Jahrling PB, Peters CJ, Stephen EL. 1984. Enhanced treatment of Lassa fever by immune plasma combined with ribavirin in cynomolgus monkeys. *J Infect Dis* 149:420–427. <http://dx.doi.org/10.1093/infdis/149.3.420>.
 9. Safronetz D, Strong JE, Feldmann F, Haddock E, Sogoba N, Brining D, Geisbert TW, Scott DP, Feldmann H. 2013. A recently isolated Lassa virus from Mali demonstrates atypical clinical disease manifestations and decreased virulence in cynomolgus macaques. *J Infect Dis* 207:1316–1327. <http://dx.doi.org/10.1093/infdis/jit004>.
 10. Wulff H, Johnson KM. 1979. Immunoglobulin M and G responses measured by immunofluorescence in patients with Lassa or Marburg virus infections. *Bull World Health Organ* 57:631–635.
 11. Safronetz D, Lopez JE, Sogoba N, Traore SF, Raffel SJ, Fischer ER, Ebihara H, Branco L, Garry RF, Schwan TG, Feldmann H. 2010. Detection of Lassa virus, Mali. *Emerg Infect Dis* 16:1123–1126. <http://dx.doi.org/10.3201/eid1607.100146>.
 12. Jahrling PB, Frame JD, Smith SB, Monson MH. 1985. Endemic Lassa fever in Liberia. III. Characterization of Lassa virus isolates. *Trans R Soc Trop Med Hyg* 79:374–379.
 13. Brining DL, Mattoon JS, Kercher L, LaCasse RA, Safronetz D, Feldmann H, Parnell MJ. 2010. Thoracic radiography as a refinement methodology for the study of H1N1 influenza in cynomolgus macaques (*Macaca fascicularis*). *Comp Med* 60:389–395.
 14. Smyth GK, Speed T. 2003. Normalization of cDNA microarray data. *Methods* 31:265–273. [http://dx.doi.org/10.1016/S1046-2023\(03\)00155-5](http://dx.doi.org/10.1016/S1046-2023(03)00155-5).
 15. Yang YH, Dudoit S, Luu P, Lin DM, Peng V, Ngai J, Speed TP. 2002. Normalization for cDNA microarray data: a robust composite method addressing single and multiple slide systematic variation. *Nucleic Acids Res* 30:e15. <http://dx.doi.org/10.1093/nar/30.4.e15>.
 16. Yang YH, Dudoit S, Luu P, Speed TP. 2001. Normalization for cDNA microarray data: microarrays, optical technologies, and informatics. *In* Bittner ML, Chen Y, Dorsel AN, Dougherty ER (ed), *Proceedings of SPIE*, vol 4266. SPIE Press, Bellingham, WA.
 17. Smyth GK. 2005. Limma: linear models for microarray data. *In* Gentleman R, Carey VJ, Huber W, Irizarry RA, Dudoit S (ed), *Bioinformatics and computational biology solutions using R and Bioconductor*. Springer, New York, NY.
 18. R Development Core Team. 2011. R: a language and environment for statistical computing. The R Foundation for Statistical Computing, Vienna, Austria.
 19. Barrett T, Troup DB, Wilhite SE, Ledoux P, Evangelista C, Kim IF, Tomashevsky M, Marshall KA, Phillippy KH, Sherman PM, Muetter RN, Holko M, Ayanbule O, Yefanov A, Soboleva A. 2011. NCBI GEO: archive for functional genomics data sets—10 years on. *Nucleic Acids Res* 39:D1005–D1010. <http://dx.doi.org/10.1093/nar/gkq1184>.
 20. Tchitchek N, Dzib JF, Targat B, Noth S, Benecke A, Lesne A. 2012. CDS: a fold-change based statistical test for concomitant identification of distinctness and similarity in gene expression analysis. *Genomics Proteomics Bioinformatics* 10:127–135. <http://dx.doi.org/10.1016/j.gpb.2012.06.002>.
 21. Fisher RA. 1922. On the interpretation of χ^2 from contingency tables, and the calculation of P. *J R Stat Soc* 85:87–94. <http://dx.doi.org/10.2307/2340521>.
 22. Benjamini Y, Hochberg Y. 1995. Controlling the false discovery rate—a practical and powerful approach to multiple testing. *J R Stat Soc B* 57:289–300.
 23. Becavin C, Tchitchek N, Mints-Eya C, Lesne A, Benecke A. 2011. Improving the efficiency of multidimensional scaling in the analysis of high-dimensional data using singular value decomposition. *Bioinformatics* 27:1413–1421. <http://dx.doi.org/10.1093/bioinformatics/btr143>.
 24. Kruskal JB, Wish M. 1978. *Multidimensional scaling*. Sage Publications, Beverly Hills, CA.
 25. Su AI, Wiltshire T, Batalov S, Lapp H, Ching KA, Block D, Zhang J, Soden R, Hayakawa M, Kreiman G, Cooke MP, Walker JR, Hogenesch JB. 2004. A gene atlas of the mouse and human protein-encoding transcriptomes. *Proc Natl Acad Sci U S A* 101:6062–6067. <http://dx.doi.org/10.1073/pnas.0400782101>.
 26. Chen EY, Tan CM, Kou Y, Duan Q, Wang Z, Meirelles GV, Clark NR, Ma'ayan A. 2013. Enrichr: interactive and collaborative HTML5 gene list enrichment analysis tool. *BMC Bioinformatics* 14:128. <http://dx.doi.org/10.1186/1471-2105-14-128>.
 27. Russier M, Pannetier D, Baize S. 2012. Immune responses and Lassa virus infection. *Viruses* 4:2766–2785. <http://dx.doi.org/10.3390/v4112766>.
 28. Mahanty S, Hutchinson K, Agarwal S, McRae M, Rollin PE, Pulendran B. 2003. Cutting edge: impairment of dendritic cells and adaptive immunity by Ebola and Lassa viruses. *J Immunol* 170:2797–2801. <http://dx.doi.org/10.4049/jimmunol.170.6.2797>.
 29. Baize S, Kaplon J, Faure C, Pannetier D, Georges-Courbot MC, Deubel V. 2004. Lassa virus infection of human dendritic cells and macrophages is productive but fails to activate cells. *J Immunol* 172:2861–2869. <http://dx.doi.org/10.4049/jimmunol.172.5.2861>.
 30. Baize S, Marianneau P, Loth P, Reynard S, Journeaux A, Chevallier M, Tordo N, Deubel V, Contamin H. 2009. Early and strong immune responses are associated with control of viral replication and recovery in Lassa virus-infected cynomolgus monkeys. *J Virol* 83:5890–5903. <http://dx.doi.org/10.1128/JVI.01948-08>.
 31. Russier M, Reynard S, Tordo N, Baize S. 2012. NK cells are strongly activated by Lassa and Mopeia virus-infected human macrophages in vitro but do not mediate virus suppression. *Eur J Immunol* 42:1822–1832. <http://dx.doi.org/10.1002/eji.201142099>.
 32. Johnson KM, McCormick JB, Webb PA, Smith ES, Elliott LH, King IJ. 1987. Clinical virology of Lassa fever in hospitalized patients. *J Infect Dis* 155:456–464. <http://dx.doi.org/10.1093/infdis/155.3.456>.
 33. Jahrling PB, Frame JD, Rhoderick JB, Monson MH. 1985. Endemic Lassa fever in Liberia. IV. Selection of optimally effective plasma for treatment by passive immunization. *Trans R Soc Trop Med Hyg* 79:380–384.
 34. Pannetier D, Reynard S, Russier M, Carnec X, Baize S. 2014. Production of CXC and CC chemokines by human antigen-presenting cells in response to Lassa virus or closely related immunogenic viruses, and in cynomolgus monkeys with lassa fever. *PLoS Negl Trop Dis* 8:e2637. <http://dx.doi.org/10.1371/journal.pntd.0002637>.
 35. Djavani MM, Crasta OR, Zapata JC, Fei Z, Folkerts O, Sobral B, Swindells M, Bryant J, Davis H, Pauza CD, Lukashevich IS, Hammamieh R, Jett M, Salvato MS. 2007. Early blood profiles of virus infection in a monkey model for Lassa fever. *J Virol* 81:7960–7973. <http://dx.doi.org/10.1128/JVI.00536-07>.
 36. Amiot L, Vu N, Rauch M, L'Helgoualc'h A, Chalmel F, Gascan H, Turlin B, Guyader D, Samson M. 2014. Expression of HLA-G by mast cells is associated with hepatitis C virus-induced liver fibrosis. *J Hepatol* 60:245–252. <http://dx.doi.org/10.1016/j.jhep.2013.09.006>.
 37. Aoki R, Kawamura T, Goshima F, Ogawa Y, Nakae S, Nakao A, Moriishi K, Nishiyama Y, Shimada S. 2013. Mast cells play a key role in host defense against herpes simplex virus infection through TNF-alpha and IL-6 production. *J Invest Dermatol* 133:2170–2179. <http://dx.doi.org/10.1038/jid.2013.150>.
 38. Becker M, Lemmermann NA, Ebert S, Baars P, Renzaho A, Podlech J, Stassen M, Reddehase MJ. 25 August 2014. Mast cells as rapid innate sensors of cytomegalovirus by TLR3/TRIF signaling-dependent and -independent mechanisms. *Cell Mol Immunol* <http://dx.doi.org/10.1038/cmi.2014.73>.
 39. Ebert S, Becker M, Lemmermann NA, Buttner JK, Michel A, Taube C, Podlech J, Bohm V, Freitag K, Thomas D, Holtappels R, Reddehase MJ, Stassen M. 2014. Mast cells expedite control of pulmonary murine cytomegalovirus infection by enhancing the recruitment of protective CD8 T cells to the lungs. *PLoS Pathog* 10:e1004100. <http://dx.doi.org/10.1371/journal.ppat.1004100>.
 40. Graham AC, Hilmer KM, Zickovich JM, Obar JJ. 2013. Inflammatory response of mast cells during influenza A virus infection is mediated by active infection and RIG-I signaling. *J Immunol* 190:4676–4684. <http://dx.doi.org/10.4049/jimmunol.1202096>.
 41. Kaiko GE, Loh Z, Spann K, Lynch JP, Lalwani A, Zheng Z, Davidson S, Uematsu S, Akira S, Hayball J, Diener KR, Baines KJ, Simpson JL, Foster PS, Phipps S. 2013. Toll-like receptor 7 gene deficiency and early-life pneumovirus infection interact to predispose toward the development of asthma-like pathology in mice. *J Allergy Clin Immunol* 131:1331–1339.
 42. Liu B, Meng D, Wei T, Zhang S, Hu Y, Wang M. 2014. Apoptosis and pro-inflammatory cytokine response of mast cells induced by influenza

- A viruses. PLoS One 9:e100109. <http://dx.doi.org/10.1371/journal.pone.0100109>.
43. Beale J, Jayaraman A, Jackson DJ, Macintyre JD, Edwards MR, Walton RP, Zhu J, Ching YM, Shamji B, Edwards M, Westwick J, Cousins DJ, Hwang YY, McKenzie A, Johnston SL, Bartlett NW. 2014. Rhinovirus-induced IL-25 in asthma exacerbation drives type 2 immunity and allergic pulmonary inflammation. *Sci Transl Med* 6:256ra134. <http://dx.doi.org/10.1126/scitranslmed.3009124>.
44. Zhu J, Message SD, Qiu Y, Mallia P, Kebabze T, Contoli M, Ward CK, Barnathan ES, Mascelli MA, Kon OM, Papi A, Stanciu LA, Jeffery PK, Johnston SL. 2014. Airway inflammation and illness severity in response to experimental rhinovirus infection in asthma. *Chest* 145:1219–1229. <http://dx.doi.org/10.1378/chest.13-1567>.
45. St John AL, Rathore AP, Raghavan B, Ng ML, Abraham SN. 2013. Contributions of mast cells and vasoactive products, leukotrienes and chymase, to dengue virus-induced vascular leakage. *eLife* 2:e00481. <http://dx.doi.org/10.7554/eLife.00481>.
46. Malhotra S, Yen JY, Honko AN, Garamszegi S, Caballero IS, Johnson JC, Mucker EM, Trefry JC, Hensley LE, Connor JH. 2013. Transcriptional profiling of the circulating immune response to Lassa virus in an aerosol model of exposure. *PLoS Negl Trop Dis* 7:e2171. <http://dx.doi.org/10.1371/journal.pntd.0002171>.